Direct Observation of Vortex Decoupling in Synthetic MoGe/Ge Multilayers

D. G. Steel,[1] W. R. White,[2] and J. M. Graybeal[1]
[1]Department of Physics, Massachusetts Institute of Technology, Cambridge, Massachusetts 02139
[2]Department of Applied Physics, Stanford University, Stanford, California 94305
(Received 26 January 1993)

Interlayer vortex decoupling is directly observed as a function of temperature and applied magnetic field via electronic transport perpendicular to the layers in a synthetic model system consisting of MoGe/Ge multilayers. Below the decoupling temperature T_D the resistivity anisotropy collapses and striking nonlinearities appear in the perpendicular current-voltage behavior, which are not observed in parallel transport. A crossover in behavior is also observed at a field H_x, in accordance with theory.

PACS numbers: 74.60.Ge, 74.76.Db, 74.80.Dm

The nature of the vortex state in layered superconductors is an area of considerable active interest. The statistical physics of the vortices is determined by issues such as dimensionality, thermal fluctuations, disorder, and interactions. The relevant vortex interactions include magnetic and Josephson interlayer couplings, as well as vortex-vortex interlayer interactions. In light of the interplay of these factors, even the most fundamental questions persist regarding the nature of the phase diagram within the vortex state. Such critical issues include the number and character of phases involved, plus which phases exhibit true zero resistance. Considering the controversy and complexity surrounding the high temperature cuprate systems, experimental examination of model systems can provide important additional insight into these issues.

In this work, we address the interlayer vortex coupling as a function of temperature T and applied magnetic field **H**. For sufficiently large anisotropy, the interlayer coupling energy between single-layer two-dimensional (2D) vortex "pancakes" becomes comparable to k_BT for an observable region near the mean-field phase boundary, resulting in a thermally driven decoupled regime. Significant controversy exists regarding the expected behavior at lower temperatures, with conflicting predictions of crossover behavior and first-order phase transitions [1-5].

While perpendicular transport is conceptually simple, it has significant qualitative and quantitative implications. We define directions with respect to the layers, with **H** *always* perpendicular ($\perp$) and applied currents either perpendicular or parallel ($\parallel$). Unlike parallel (in-plane) transport, perpendicular transport directly probes the interlayer phase coupling [6,7]. In this "Lorentz force-free" orientation, the current does not couple to rigid line vortices in linear response.

In a finite-field regime near the mean-field critical field H_{c2}^{MF}, we observe a perpendicular resistivity $\rho_\perp$ equal to the normal-state value $\rho_{\perp N}$, showing that the layers are decoupled and the vortices are 2D in nature. As T is lowered below a temperature $T_D(H)$ an abrupt drop in $\rho_\perp$ is found, corresponding to the buildup of interlayer phase coupling and the establishment of line vortices. Unlike perpendicular transport in high-T_c single crystals, no upturn in $\rho_\perp$ is observed below T_c [8]. Substantial nonlinearities also appear. In contrast, the in-plane transport response remains linear with a finite resistance as we pass through T_D, indicating that the transition is not associated with in-plane ordering.

We chose a synthetic model system for this study, amorphous a-MoGe/Ge multilayers. This system has proven merits and is compatible with photolithographic techniques [9-12]. The samples consisted of ten 2D superconducting 60-Å-thick layers of a-$Mo_{77}Ge_{23}$ alternating with $d_{\mathrm{Ge}}=65$ Å layers of insulating a-Ge, so the periodicity $s=125$ Å. One sample set was reactive-ion etched (RIE) into 20-μm-wide bridges for transport parallel to the layers. Perpendicular transport samples (Fig. 1, lower inset) had additional 1250 Å and 500 Å MoGe bottom and top contact layers, and were patterned into pedestals of area $\mathcal{A}=(200\ \mu\mathrm{m})^2$. Leads were wire bonded to the contact layers. The presence of electronic disorder lowers the T_c of the 2D layers by ~ 2 K relative to the thicker contact layers [10]. Stopping the RIE on

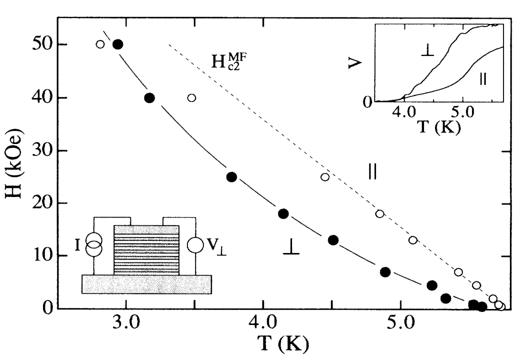

FIG. 1. The interlayer decoupling temperature T_D (●) as obtained from perpendicular transport using midpoint criteria; solid line is to guide the eye. Also shown are the in-plane resistive midpoint (○) and mean field $H_{c2}^{\mathrm{MF}}(T)$. Inset at upper right contrasts parallel and perpendicular traces for $H=13$ kOe. A schematic of the perpendicular transport geometry is shown at lower left.

0031-9007/93/71(1)/161(4)$06.00

the bottom layer created a four-probe geometry where modest currents perpendicular to the layers induced no observable dissipation in the more robust contact layers.

Unlike high-T_c materials, these multilayers contain no extended defects such as twin planes, grain boundaries, or intergrowths. The effective mass anisotropy $\gamma^2 \equiv \lambda_\perp^2/\lambda_\parallel^2$, the squared ratio of the interlayer to intralayer penetration lengths, is $\sim 10^3$ and thus comparable to the $Bi_2Sr_2CaCu_2O_8$ high-T_c system. This value is extrapolated from γ^2 values for multilayers with 5 Å $< d_{Ge} <$ 45 Å, obtained from the fluctuation conductivity dimensional crossover [13]. The penetration length for MoGe is 8000 Å [9].

Measurements were made in a screened room using a superconducting magnet. All sample leads were electrically filtered. Separate in-plane and pedestal samples allowed simultaneous measurement of the parallel and perpendicular transport. The $T_c(H=0)$'s for in-plane and perpendicular transport were sharp and identical within sample-to-sample variations of ~ 0.1 K. The measured normal-state resistances ($R_{\parallel N} \approx 2$ kΩ, $R_{\perp N} \approx 0.2$ Ω) yield a resistivity anisotropy $\rho_{\perp N} \simeq 4 \times 10^4$. $R_{\perp N}$ is consistent with estimates based on the known tunneling length of 8.1 Å for *a*-Ge [13], and was observed to scale inversely with $\mathcal{A}$. The measured zero-field critical currents were finite with nonhysteretic *I-V* characteristics down to 2 K [$I_c(2\text{ K}) \approx 1$ mA], as expected from the calculated McCumber parameter. This argues strongly against pinholes within the Ge layers dominating the perpendicular transport, as local hot-spot formation would result in substantial hysteresis.

The upper inset of Fig. 1 shows temperature sweeps for in-plane and perpendicular transport at $H=13$ kOe. As T is lowered, first the in-plane resistance $R_\parallel(T)$ begins to drop. Using a resistive midpoint criterion, the resultant mean-field critical field slope is consistent with the coherence length for MoGe. At finite fields, $R_\parallel(T)$ decreases but remains finite at lower T due to vortex diffusion. Other than modest edge pinning [11], linear response was observed for in-plane current densities of $10^{-3} < J < 10^2$ A/cm^2.

In contrast, the perpendicular voltage $V_\perp(T)$ remains constant and independent of H as one passes through $H_{c2}^{\rm MF}(T)$, corresponding to the normal-state resistivity $\rho_{\perp N}$. It then drops sharply at a lower temperature T_D. As shown in Fig. 1, the measured field dependence of T_D differs markedly from that of $H_{c2}^{\rm MF}$, approaching it for $H > 50$ kOe. The measurement current was $I=1$ μA, corresponding to the low current density $J=2.5\times10^{-3}$ A/cm^2. Even then, linear response was generally not observed for $V_\perp \lesssim 0.5 V_{\perp N}$. Hence $V_\perp$ vs T traces at fixed I yield an upper bound on $R_\perp(T)$, with the actual resistive transition being sharper. No hysteresis was observed for either current direction.

To explore the perpendicular transport nonlinearities, we turned to dc I-$V_\perp$ characteristics. At zero field we observed a sharply defined critical current I_c for $T < T_c$, the mean-field transition temperature. However, as the field is increased to 1 kOe, a smoothly varying nonzero voltage progressively appears below the jump at "I_c." At a characteristic field $H_x \approx 700$ Oe, the sharp jump at I_c disappears, leaving a smooth upward-curving I-$V_\perp$ for higher H.

To best display the perpendicular nonlinearities for $H > H_x$, we measured the differential resistance $\partial V_\perp/\partial I$ vs I using a variable dc current I plus a small ac component δI_{ac} (1 μA), detecting the ac voltage with a lock-in. Representative curves taken at various T for $H=18$ kOe are shown in Fig. 2. The high temperature behavior shows Ohmic response, but as the temperature is lowered through T_D strong nonlinearities appear. First a sharp "cusp" appears, whose current scale (~ 5 μA) is relatively independent of temperature or field for $H > H_x$. Note that the bottom of the cusp is rounded by the finite ac current amplitude δI_{ac} so we do not observe linear response even at zero dc current. Upon further lowering T, the cusp deepens and added curvature appears at higher currents. This high-bias behavior is consistent with a power-law dependence (Fig. 2 inset). At lower T only the power-law behavior remains. Writing $\partial V_\perp/\partial I \propto I^{\alpha-1}$, α increases with decreasing T with $1.2 \le \alpha \le 2.2$ in our measured range. Recall that no low-bias nonlinearities were observed in the in-plane transport either above or below T_D.

It is also interesting to observe the temperature dependence of the resistivity anisotropy as we pass through T_D. Over most of the range we observe nonlinear perpendicular transport, so our measurements yield an upper bound for the true perpendicular resistivity $\rho_\perp(T)$. From the measured voltage, we thus define a *current-dependent* quantity

$$\rho_\perp^{\rm ub}(T) \equiv \frac{V_\perp}{I}\frac{\mathcal{A}}{10s},$$

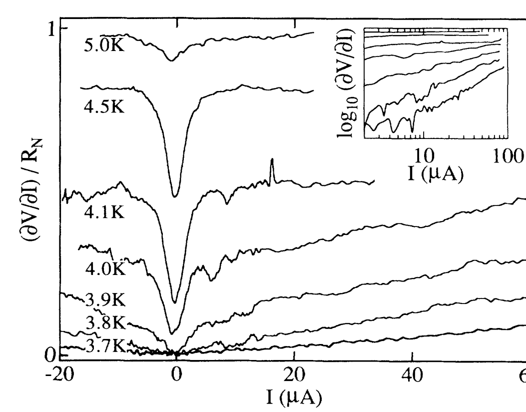

FIG. 2. Normalized perpendicular differential resistance vs current for a sequence of temperatures, measured at 19 kOe with an ac modulation current $\delta I_{ac}=1$ μA. Inset shows a log-log plot of the high-bias data, which are consistent with power-law behavior.

such that $\rho_\perp^{ub}(T) \geq \rho_\perp(T)$. For our voltage sensitivity (200 pV) we extend $\rho_\perp^{ub}$ to lower values by increasing I and going further into the nonlinear regime. Figure 3 shows the data for three perpendicular currents. At the lowest of these currents, $\rho_\perp^{ub}$ drops sharply near the temperature where $\rho_\parallel$ exhibits a "kink," which has been shown [12] to arise from the onset of interlayer correlation of the vortex motion. While the normal-state resistivity anisotropy is 4×10^4, we observe that below T_D the anisotropy drops by more than four decades and is *at most* of order unity at low T. Because $\rho_\parallel(T)$ remains finite below T_D and in linear response, T_D is clearly not coincident with an in-plane melting transition. The vortices remain mobile in each superconducting layer, but the motion in different layers is coupled below T_D.

Let us reflect upon the results. For $H < H_{c2}^{MF}$ and $T > T_D$ the measured $\rho_\perp(H,T)$ is equal to the normal-state value $\rho_{\perp N}$, so we conclude via the Josephson relation that the relative phases of the layers are incoherent. Hence, this regime corresponds to decoupled 2D layers. As we cool below $H_{c2}^{MF}(T)$ the 2D correlation length ζ_{2D} within each layer grows, ultimately diverging at the 2D melting transition T_m^{2D}, estimated to be ~2 K [14,15]. The presence of disorder will cut off this divergence [16]. For $\gamma^2 = 10^3$ the dominant interlayer coupling is via the Josephson term, with energy density E_J [1,4]. We can thus estimate the intralayer correlation length ξ_+ just above T_D via the relation $E_J\xi_+^2 \sim k_BT$, i.e., when the intralayer correlations grow to such a scale that interlayer Josephson coupling of correlated regions can occur. From this criterion we obtain ξ_+/a to be of order ~ 1–10 for our measured points (a is the vortex spacing), e.g., at $H=10$ kOe, $\xi_+ \sim 0.2$ μm. Such short correlation lengths are consistent with T being well above T_m^{2D}, or with static disorder setting the translational correlation length.

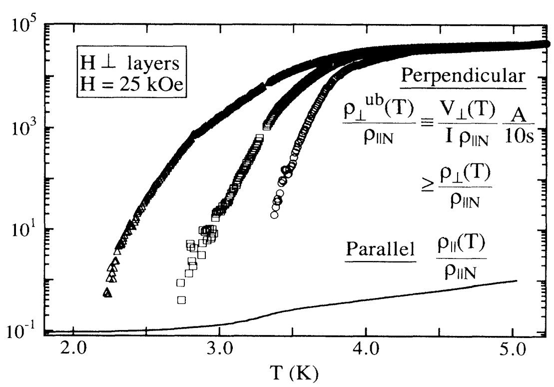

FIG. 3. The in-plane resistivity $\rho_\parallel$ and the measured *upper bound* on the perpendicular resistivity $\rho_\perp^{ub}$ as functions of temperature at 25 kOe. Values are normalized to the in-plane normal-state value $\rho_{\parallel N}$. $\rho_\perp^{ub}(T)$ is shown for three different currents (right to left: 3, 67, 333 μA) which progressively delve deeper into nonlinear response. Note the rapid drop in the resistivity anisotropy, and the absence of sharp features in the in-plane response.

In the regime $T < T_D$, we note that the characteristic field H_x separating the two I-V behaviors is numerically close to the predicted crossover field $H_{cr} \approx 2\pi\phi_0/\gamma^2 s^2 = 830$ Oe [1–5], although definitions vary by small factors. Here ϕ_0 is the magnetic flux quantum. H_{cr} is set by the length γs, the scale on which the energy for interlayer vortex displacements crosses over from quadratic to linear dependence due to the formation of Josephson "strings." For $H < H_{cr}$ single line vortex behavior is expected, whereas above H_{cr} more collective behavior is anticipated [1].

The onset of interlayer phase coupling was coincident with the appearance of nonlinearities in perpendicular transport. The observed upper bound for the onset of nonlinearities for $H > H_x$ was the minimum measurement current I_m. Assuming a *uniform* current density, $J_m = I_m/\mathcal{A} = 2.5\times10^{-3}$ A/cm^2. As such nonlinearities provide insight into the relevant length scales and excitations, their correct interpretation is critical to understanding the coupled regime. Since no in-plane nonlinearities were observed, here we consider loop excitations between layers which couple strongly to perpendicular currents. Of course, other excitations may be possible.

First we consider current-induced nucleation of vortex loops with size L. The energy of such a loop would be $E \approx \varepsilon_l \pi L - J\phi_0 L^2/c$, where ε_l is the vortex line energy [17]. Note that we use the zero-field value of γ in our evaluation of ε_l. As such loops grow they would intersect with line vortices, and this might represent a vortex line crossing process. Setting $E \approx k_BT$ and $J = J_m$ we would obtain $L \sim 10$ Å for $H > H_x$, thus $L \ll a$ over the measured field range. Although we have ignored bending terms and the influence of the background vortices, $J_m\phi_0L^2/c \ll \varepsilon_l\pi L \approx k_BT$. So even if small vortex loops are thermally nucleated, the current has negligible coupling to them and it would thus be difficult to produce the observed nonlinearities.

We now consider the possibility of collective displacement loops of area L^2. As before, the interaction energy of such a loop with an applied current would be $E_I \sim J\phi_0L^2/c$. However, their cost of formation may grow more slowly than L^2 [18]. In the context of our results, we simply ask what loop size would be required such that J_m could induce nonlinearities at a temperature T. From $E_I \approx k_BT$, we obtain a substantial length scale $L \sim 30$ μm ($L/a \sim 10^3$) for uniform currents, which is numerically close to $\lambda_\perp = \gamma\lambda_\parallel$. To speak meaningfully of such a loop would require that the correlation length $\xi_- \geq L$ for $T < T_D$. Assuming uniform currents thus suggests that the correlation length jumps at T_D, as for a first-order transition. Indeed, the recent calculation of Daemen *et al.* [5] predicts a first-order decoupling transition for our value of γ^2. However, they also point out that γ is field dependent, whereas our estimate of the loop size is calculated using the zero-field value. Alternatively, if the perpendicular current is confined to the pedestal edges due to a finite supercurrent or edge pinning of the loops, then the local edge current density would be larger. Both this locally higher J or a field-enhanced γ would reduce the correlation lengths estimated here. More experiments are required to clarify this issue.

Expressing our results in terms of the decoupling field as a function of temperature, $H_D(T)$, we can compare the functional dependence with theoretical calculations for layered superconductors. Daemen *et al.* [5] predict a first-order transition with $H_D(T)=C(1/T-1/T_c)$, where $C=[\phi_0^3/16e\pi^3k_Bs\gamma^2\lambda^2(0)]\approx 1.8\times 10^6$ Oe K for our sample. While their functional form fits our data well, the fit yields a value for C roughly 60 times larger. Glazman and Koshelev [1] predict a phase transition at high fields with the destruction of the vortex lines, although their predicted functional form in this limit does not fit our results well. However, our results may be too near the crossover regime.

In conclusion, we have directly observed interlayer vortex decoupling via perpendicular transport. At high temperatures, the system consists of independent decoupled 2D layers. As the temperature is reduced, interlayer phase coupling occurs at a temperature T_D. Substantial nonlinearities in the perpendicular transport simultaneously appear, suggesting the presence of a phase transition. Below T_D, we observe a precipitous collapse in the transport anisotropy, with the resistivity perpendicular to the layers becoming at most comparable to the in-plane resistivity. A crossover in behavior is also observed at a field H_x, in accordance with theory. While the full resolution of the transport nonlinearities requires further consideration, it should be clear that they impact issues critical to the nature of the low-temperature coupled state. This insight is separate from and complementary to inplane transport results.

The authors acknowledge useful conversations with M. Beasley, J. Clem, D. Fisher, L. Glazman, A. Koshelev, and D. Nelson. This work was supported by ONR under Grant No. N00014-88-K-0479 and by NSF/DMR under Grant No. DMR 90-22933.

[1] L. I. Glazman and A. E. Koshelev, Phys. Rev. B **43**, 2835 (1991).

[2] M. V. Feigel'man, V. B. Geshkenbein, and V. M. Vinokur, Pis'ma Zh. Eksp. Teor. Fiz. **52**, 1141 (1990) [JETP Lett. **52**, 546 (1990)].

[3] S. Ryu, S. Doniach, G. Deutscher, and A. Kapitulnik, Phys. Rev. Lett. **68**, 710 (1992).

[4] D. S. Fisher, in *Phenomenology and Applications of High Temperature Superconductors,* edited by K. Bedell *et al.* (Addison-Wesley, Reading, MA, 1992).

[5] L. L. Daemen, L. N. Bulaevskii, M. P. Maley, and J. Y. Coulter, Phys. Rev. Lett. **70**, 1167 (1993).

[6] R. Busch, G. Ries, H. Werthner, G. Kreiselmeyer, and G. Saemenn-Ischenko, Phys. Rev. Lett. **69**, 522 (1992).

[7] H. Safar, E. Rodriguez, F. de la Cruz, P. L. Gammel, L. F. Schneemeyer, and D. J. Bishop, Phys. Rev. B **46**, 14238 (1992).

[8] G. Briceño, M. F. Crommie, and A. Zettl, Phys. Rev. Lett. **66**, 2164 (1991).

[9] N. Missert, Ph.D. thesis, Stanford University, 1989 (unpublished).

[10] J. M. Graybeal and M. R. Beasley, Phys. Rev. B **29**, 4167 (1984).

[11] W. R. White, A. Kapitulnik, and M. R. Beasley, Phys. Rev. Lett. **70**, 670 (1993).

[12] W. R. White, A. Kapitulnik, and M. R. Beasley, Phys. Rev. Lett. **66**, 2826 (1991).

[13] S. T. Ruggiero, Ph.D. thesis, Stanford University, 1981 (unpublished); S. T. Ruggiero, T. W. Barbee, and M. R. Beasley, Phys. Rev. Lett. **45**, 1299 (1980).

[14] D. S. Fisher, Phys. Rev. B **22**, 1190 (1980).

[15] S. W. de Leeuw and J. W. Perram, Physica (Amsterdam) **113A**, 546 (1982). Their results imply the factor $A \simeq 0.65$ in Ref. [14].

[16] A. Yazdani, W. R. White, M. R. Hahn, M. Gabay, M. R. Beasley, and A. Kapitulnik, Phys. Rev. Lett. **70**, 505 (1993).

[17] J. R. Clem, M. W. Coffey, and Z. Hao, Phys. Rev. B **44**, 2732 (1991).

[18] D. S. Fisher, M. P. A. Fisher, and D. A. Huse, Phys. Rev. B **43**, 130 (1991).